

# Nonhysteretic Phenomena in the Metal–Semiconductor Phase-Transition Loop of VO<sub>2</sub> Films for Bolometric Sensor Applications

Michael Gurvitch, Serge Luryi, *Fellow, IEEE*, Aleksandr Polyakov, and Alexander Shabalov

**Abstract**—Hysteresis observed in the resistive semiconductor-to-metal phase transition in VO<sub>2</sub> causes problems in bolometric readout, and thus is an obstacle in utilizing this strong phase transition in bolometric sensor applications. It is possible to avoid the unwanted hysteresis when operating in limited temperature ranges within the hysteresis loop of VO<sub>2</sub>. Nonhysteretic branches (NHB-s) traced in such limited temperature intervals turned out to have much higher temperature coefficient of resistance (TCR) than VO<sub>2</sub> at room temperature: while TCR at 25 °C in VO<sub>2</sub> is close to 3%, peak TCR values in NHB-s reach 6% in VO<sub>2</sub> films on Si/SiO<sub>2</sub> substrates and 21% in films on crystalline sapphire substrates. At the same time, the nanoscopic-scale mixture of semiconducting and metallic phases in VO<sub>2</sub> within its hysteresis loop provides for partially shunted low resistivity, thus creating an unprecedented combination of record high semiconducting TCR and metal-like low resistance. This combination may benefit the uncooled focal plane array microbolometer IR visualization technology.

**Index Terms**—Bolometers, hysteresis, image sensors, metal-insulator transition, vanadium dioxide.

## I. INTRODUCTION

UNCOOLED focal plane array (UFPA) IR visualization technology utilizes microbolometer sensors consisting of a mixed oxide VO<sub>x</sub> [1]–[4]. Pure oxide VO<sub>2</sub> is not utilized in this technology primarily because of the readout problems arising in the presence of resistive hysteresis [5], [6], as discussed in Section II. While mixed, nonstoichiometric semiconducting oxide VO<sub>x</sub> can be prepared so as to avoid hysteresis, and thus, mitigate said readout problems, its temperature coefficient of resistance (TCR)  $\equiv (1/R)dR/dT$  is relatively low, rarely exceed-

ing 2% °C<sup>-1</sup> [1]–[5]. Addressing this problem, we found that hysteresis could be avoided in VO<sub>2</sub>, in limited temperature intervals of 5–6 °C inside its major hysteresis loop, in what we called the *nonhysteretic branches* (NHB-s) [7]–[9]. We have also found that in these NHB-s the TCR can be significantly increased compared to the room-temperature semiconductor TCR found in VO<sub>x</sub> and VO<sub>2</sub>. The appearance of NHB-s and enhanced TCR-s required an explanation, which was provided [7]–[9] by a qualitative, percolation-based picture. We will briefly revisit this explanation here in Section IV. In addition to explaining the appearance of NHB-s, our picture accounts for the observed resistive-optical correlations [8], [9]. We proposed [7]–[9] to utilize NHB regime for the benefit of UFPA technology. In addition to the hysteresis-free operation, there are two major arguments in favor of this approach:

- 1) enhanced TCR values in NHB-s;
- 2) ability to lower pixel resistance by orders of magnitude while maintaining high TCR.

We previously found [8], [9] that it is possible to combine TCR of about 4% °C<sup>-1</sup> with values of pixel resistance  $R$  as low as 20 Ω. This can benefit UFPA technology, especially in view of both Johnson and  $1/f$  noise decreasing with lower  $R$ . In contrast, pixel resistances in today's UFPA technology are between 10 and 50 kΩ, 500 to 2500 times higher. The primary reason for using high-resistance pixels in existing VO<sub>x</sub> sensor technology is that at a lower resistance, the TCR decreases to unacceptably small values. This is not so in a NHB regime, which makes it especially appealing. The advantages and disadvantages of the NHB regime were discussed in some detail in [8].

Here, we would like to present new data recently obtained with better quality VO<sub>2</sub>. We found NHB behavior described previously [7]–[9] albeit in more narrow temperature intervals of  $\approx 2$  °C. The remarkable fact we wish to present here is that in this better quality VO<sub>2</sub>, TCR in NHB regime can reach 21% °C<sup>-1</sup>, a value unseen in any other nonhysteretic semiconducting bolometer.

## II. HOW HYSTERESIS CAUSES PROBLEMS IN BOLOMETRIC READOUT: FORWARD AND BACKWARD EXCURSIONS

Before we present our NHB data, we would like to introduce the hysteretic phase transition found in VO<sub>2</sub> films and to discuss the aforementioned bolometric readout problem caused by hysteresis.

A bolometer reacts to a temperature change  $\Delta T$  by changing its resistance by  $\Delta R$ . The larger is  $\Delta R$  for a given  $\Delta T$ , the

Manuscript received December 20, 2009; revised March 22, 2010; accepted March 25, 2010. Date of publication April 19, 2010; date of current version September 9, 2010. This work was supported by the New York State Foundation for Science, Technology, and Innovation through the facilities of the Center for Advanced Sensor Technology at Stony Brook. The review of this paper was arranged by Associate Editor E. Towe.

M. Gurvitch is with the Department of Physics and Astronomy, State University of New York at Stony Brook, Stony Brook, NY 11794 USA and also with the New York State Center for Advanced Sensor Technology (Sensor CAT) at Stony Brook (e-mail: michael.gurvitch@sunysb.edu).

S. Luryi is with the Department of Electrical and Computer Engineering, State University of New York at Stony Brook, Stony Brook, NY 11794 USA and also with the New York State Center for Advanced Sensor Technology (Sensor CAT) at Stony Brook (e-mail: serge.luryi@stonybrook.edu).

A. Polyakov and A. Shabalov are with the New York State Center for Advanced Sensor Technology, State University of New York, Stony Brook, NY 11794 USA (e-mail: apolyakov@notes.cc.sunysb.edu; sasha@ece.sunysb.edu).

Color versions of one or more of the figures in this paper are available online at <http://ieeexplore.ieee.org>.

Digital Object Identifier 10.1109/TNANO.2010.2047867

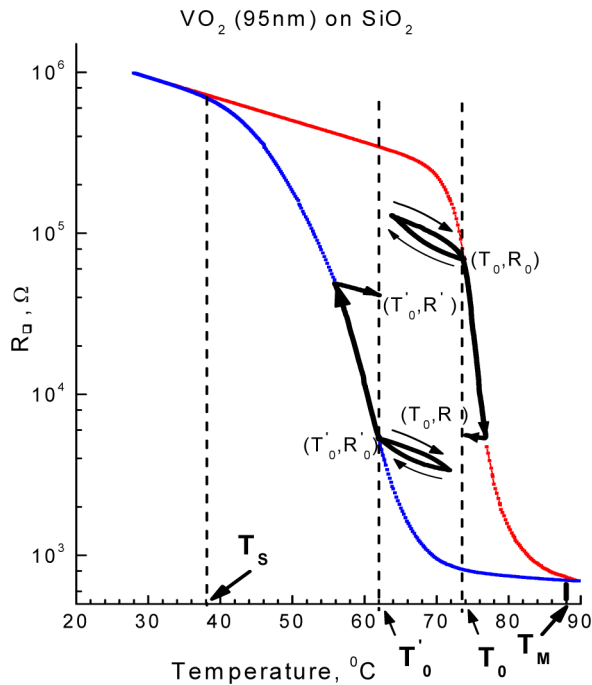


Fig. 1. Forward and backward excursions originating from points  $(T_0, R_0)$  on a HB and  $(T'_0, R'_0)$  on a cooling branch. (Note that this figure is not a schematic drawing, it shows the measured loops and parts of loops on a 95 nm  $\text{VO}_2$  deposited on  $\text{Si}/\text{SiO}_2$  substrate by PLD method.)

greater is the sensitivity. At the same time, very large resistance  $R$  is detrimental [1]–[4] because of the Joule heating during the bolometric sensor readout, the difficulty of the electronic readout circuit matching, and the higher noise, both Johnson's and  $1/f$ . Thus, a balanced figure of merit for a bolometric material is the TCR, which evaluates  $(\Delta R/R)/\Delta T$  rather than  $\Delta R/\Delta T$ . It may appear that the steep semiconductor to metal transition in  $\text{VO}_2$  [10], [11], as shown in Fig. 1 for a 95 nm film, might offer the greatest sensitivity (high TCR). It is, however, hysteretic. Let us look in more detail on how hysteresis causes problems. To be specific, consider a bolometer positioned at a working point  $(T_0, R_0)$  on a steep heating branch (HB) (it will require a temperature controller to keep it at  $T_0$  above room temperature) and let it experience an influx of energy (this could be an IR signal), which momentarily heats it up, increasing its temperature by  $\Delta T$  and decreasing its resistance by a large  $\Delta R$  (see Fig. 1).

Once the heat input has been removed (which happens in resistive bolometers used in IR visualization at least 30 times per second), the bolometer returns back to the temperature  $T_0$ , however, because of the hysteresis, the  $(T, R)$  path on the way back differs from the path in the forward direction: the resistance will not come back to  $R_0$ , but instead will move along a *minor loop* to a point  $(T_0, R)$  as indicated in Fig. 1. If a bolometer will now experience a subsequent, second heat pulse, the result will be very different. This cannot be tolerated in a bolometric sensor subject to a train of pulses. In order to avoid this problem, the bolometer should be reset after each pulse, which can only be done by going all the way out of the hysteresis loop, reaching temperatures either below  $T_S$  or above  $T_M$ . While such reset-

ting can be done, it requires large temperature *excursions* (we shall refer to as an *excursion* any round-trip temperature change  $T_0 \rightarrow T_0 \pm \Delta T \rightarrow T_0$ ), followed each time by a temperature stabilization at the working point  $T_0$ . With bolometers receiving signals with frequency of 30–60 Hz (video rates), this is not practical. The problem with the different return path, we just outlined, has been described in [6], and the readout problems caused by hysteresis were acknowledged [5] as the major contributing factor in abandoning pure phase  $\text{VO}_2$ .

If temperature of the initial part of an excursion changes in the same direction as the major loop progression, we call it a *forward excursion*; if it starts in the opposite direction, it is a *backward excursion*. Because of the hysteresis, forward and backward excursions produce dramatically different results. While a forward excursion  $T_0 \rightarrow T_0 + \Delta T \rightarrow T_0$  on a HB traces an *open curve* from  $(T_0, R_0)$  to  $(T_0, R)$ , a backward excursion  $T_0 \rightarrow T_0 - \Delta T \rightarrow T_0$  produces a *closed minor loop*, which has a much gentler slope in the vicinity of  $(T_0, R_0)$  than the steep slope on the major loop. The gentle slope goes steeper for larger  $\Delta T$ , as seen in Fig. 1. This slope variation would introduce a  $\Delta T$ -dependent TCR; in other words, it would introduce a signal non-linearity in  $\log(R)$  versus  $T$ . Similar processes take place on a cooling branch (CB) (see Fig. 1), except that in this case decreasing temperature corresponds to the forward direction, and increasing temperature to the backward direction.

These problems provide an incentive to avoid hysteresis in bolometric applications. One way to avoid these problems is to use a sensor material without hysteresis, such as  $\text{VO}_x$ . Another way is to use hysteretic sensor material, but work in a NHB regime, as described in subsequent sections.

### III. NHB-S IN $\text{VO}_2$ FILMS WITH MODERATE-STRENGTH TRANSITION

Here, we present data on a 95 nm  $\text{VO}_2$  film deposited at 650 °C by pulsed laser deposition (PLD) onto a  $\text{Si}/\text{SiO}_2$  substrate [8], [9]. Transition strength can be characterized by a resistance ratio  $\text{RR} = R(25^\circ\text{C})/R(90^\circ\text{C})$ ; this film has  $\text{RR} = 1430$ . In studying minor loops in such films, we discovered [7] that for sufficiently small excursions minor loops tend to flatten out, degenerating into NHB-s, as can be seen in Fig. 2, where a number of excursions with  $\Delta T = 5^\circ\text{C}$  are shown attached to the major loop at regular intervals.

TCR-s of various NHB-s from Fig. 2 are plotted versus  $T$  (here  $T$  is the *attachment* temperature of a NHB to the major loop) in Fig. 3 for both HB and CB, together with TCR-s evaluated on the sides of the major loop.

As we see in Fig. 3, TCR-s characterizing the overall hysteretic transition start at  $\approx 3\%$  at low temperatures, rising to  $40\%^\circ\text{C}^{-1}$  and to  $125\%^\circ\text{C}^{-1}$  on the steep CB and HB sides of the major loop. TCR-s in different NHB-s also start at  $\approx 3\%$ , rising to  $4\%^\circ\text{C}^{-1}$  and  $6\%^\circ\text{C}^{-1}$  on the CB and HB. All TCR-s are decreasing to near zero at the temperatures above the transition. Further, as is evident from Fig. 3, TCR peaks on major loop and on NHB-s coincide to within  $\approx 3^\circ\text{C}$  on both branches.

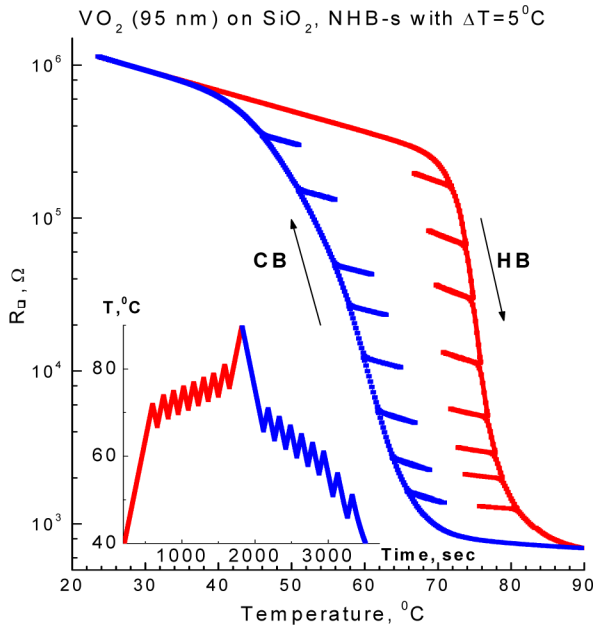


Fig. 2. Minor loops with  $\Delta T = 5^\circ\text{C}$  degenerating into NHB-s; the inset shows the way in which temperature was changed in this measurement.

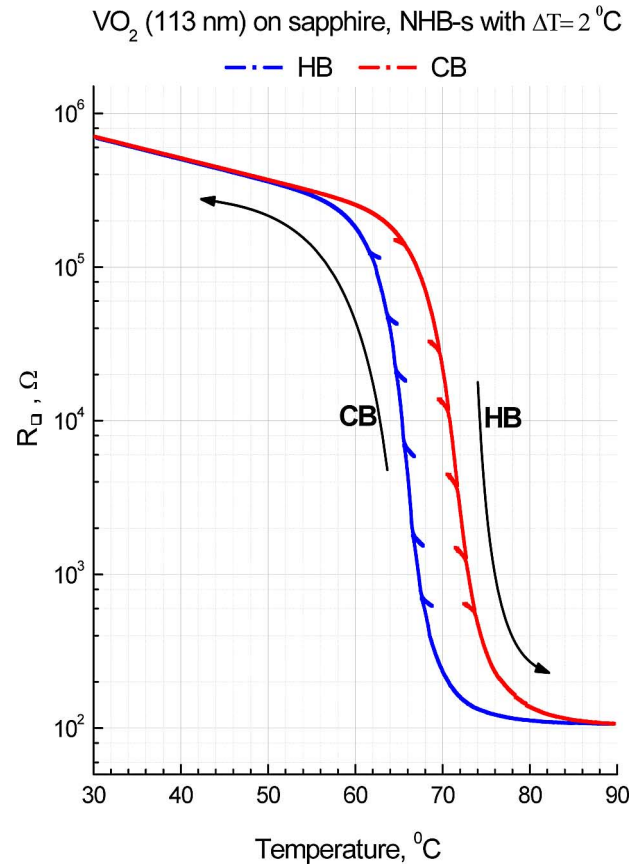


Fig. 4. NHB-s with  $\Delta T = 2^\circ\text{C}$ , 113 nm VO<sub>2</sub> film on sapphire, and RR = 8700.

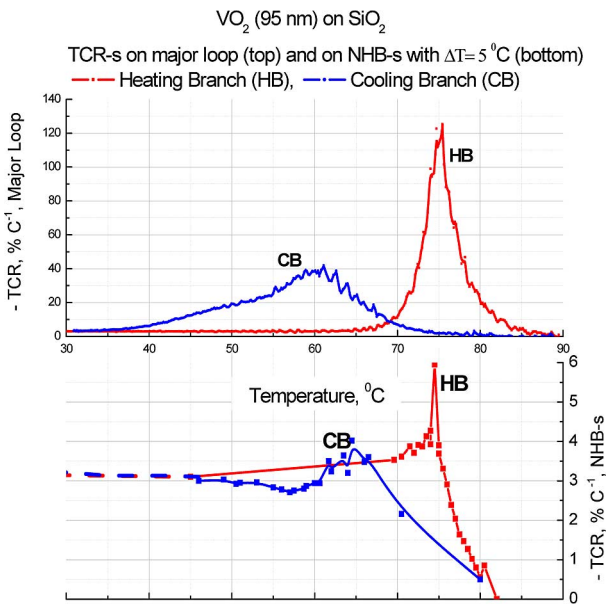


Fig. 3. TCR versus  $T$  on the sides of the major loop (two upper curves) and in various NHB-s around the major loop (two lower curves); the same sample as in Figs. 1 and 2.

#### IV. NHB-S IN VO<sub>2</sub> FILMS WITH STRONG TRANSITION

VO<sub>2</sub> films with sharper and stronger transitions than those presented in the previous section were prepared at 650 °C by PLD method on R-cut sapphire substrates. The major loop with  $\Delta T = 2^\circ\text{C}$  NHB-s is shown in Fig. 4; this sample has RR = 8700.

It was necessary to reduce  $\Delta T$  to 2 °C in order to have single-valued NHB-s in this case. In Fig. 5, we show TCR-s of this sample, both for NHB-s and for the sides of the major loop. The

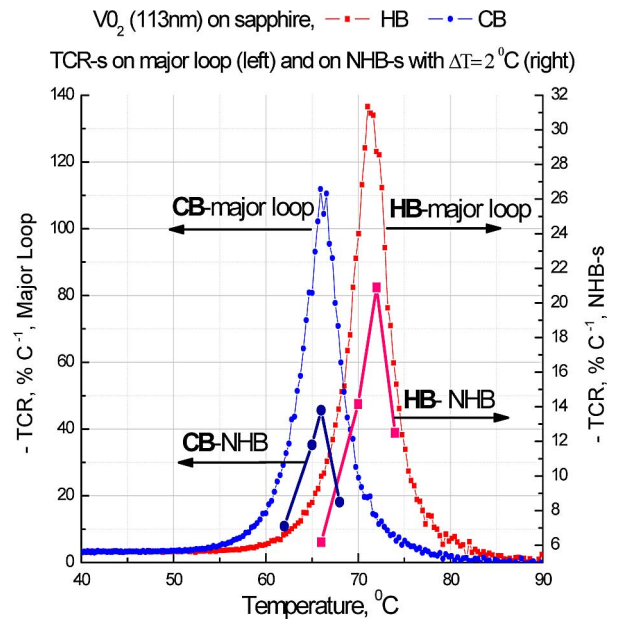


Fig. 5. TCR versus  $T$  on the sides of the major loop (two upper curves, left scale) and in NHB-s around the major loop (two lower curves, right scale); the sample is the same as in Fig. 4.

TCR values on the sides of the major loop are as high as 110% and 135%, on the CB and HB, respectively. The TCR-s of the NHB-s in this case are also exceptionally high, reaching values

of 13.6% and 21% in two sharp peaks coinciding in temperature with the major loop peaks.

## V. THEORETICAL INTERPRETATION

The hysteretic region in VO<sub>2</sub> is a mixed state comprising both S-phase and M-phase regions or domains. Each such domain located in a film around a point with spatial coordinates  $(x, y)$  transitions into the other phase at its own temperature  $T_C(x, y)$ , the variation in  $T_C$  arising from nonuniformities of composition, variations in the local strain, etc. Thus, in a macroscopic sample  $T_C(x, y)$  is quasi-continuously distributed. We assume that the local transition within a domain is sharp, further, we assume that a uniform isolated domain would transition without a hysteresis; in this we differ from much of the VO<sub>2</sub> hysteresis literature [12] in which it is usually assumed that each domain, in addition to  $T_C$ , has its own coercive temperature and a rectangular hysteresis loop. In contrast, we do not see a need for postulating such intrinsic hysteresis in isolated domains, but attribute the origin of hysteresis to the boundary energy, which affects the way domains merge and disconnect. We note that VO<sub>2</sub> single crystals have very small hysteresis [13], it seems natural to extrapolate this to the case of an ideally uniform microscopic (or nanoscopic) region, which would have zero hysteresis. In this picture, hysteresis is the result of interaction between different phases in a multidomain macroscopic sample.

At a given temperature  $T$  inside the major hysteretic loop, some parts of the film have  $T_C(x, y) < T$  and others  $T_C(x, y) > T$ . In the first approximation, the boundary wall between the S and M phases is determined by the condition  $T_C(x, y) = T$ . In this approximation, the wall is highly irregular and its ruggedness corresponds to the scale at which one can define the local  $T_C(x, y)$ , i.e., to the characteristic length scale of the nanoscopic phase domains. On closer inspection, however, we need a refinement that takes into account the *boundary energy*, associated with the phase domain wall itself. The boundary energy is positive and to minimize its contribution to the free energy, the domain walls are relatively smooth. Let us examine the process of boundary motion. For concreteness, let us consider the HB. Below the percolation transition, the M-phase resembles lakes in the S-phase mainland. With the rising temperature, the area of the M-phase increases, lakes grow in size. When a boundary of a given lake is far from the other lakes, infinitesimal  $\delta T$  changes boundary length by infinitesimal amount, and the lake area by  $\delta A_M$ . However, when the lakes are sufficiently separated, we envision a continuous, reversible, hysteresis-free process of  $M \leftrightarrow S$  area redistribution, with neighboring configurations differing *microscopically*. Let us now look at the formation of a link between two neighboring regions, which is the elementary step in the topological evolution of a global percolation picture. Let us focus on two metallic lakes that are about to merge. Since the boundary is smooth, at some temperature the distance between the lakes becomes smaller than the radius of curvature of either lake at the point they will eventually touch. Therefore, at some  $T$  the following two configurations will have equal energies: one comprising two disconnected M-phase lakes that are near touching, but not quite, and the other with a finite link formed, in Fig. 6(a) and (b), respectively.

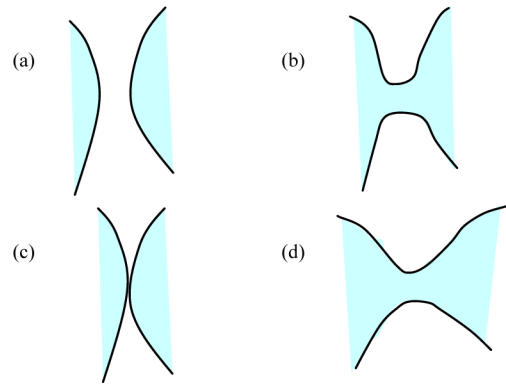


Fig. 6. Semiconductor–metal boundary; metallic phase is shown shaded. Top row (a) and (b) corresponds to temperature  $T$  and the bottom row (c) and (d) to a higher temperature  $T_0 = T + \Delta T^*$ .

Both configurations are characterized by equal boundary lengths, and therefore, have equal free energy. The actual transition forming a local link, however, does not occur at that temperature because of an immense *kinetic* barrier between these two *macroscopically* different configurations. The transition occurs at a higher  $T_0 = T + \Delta T^*$  when it is actually forced, i.e., when the two phases touch at a point. Here,  $\Delta T^*$  is the *coercive* temperature. In Fig. 6, coercive temperature arises as a result of having a boundary between different phases, it does not pre-exist intrinsically within each domain. We associate the steep slopes of the major loop with the quasi-continuous formation of such links, i.e., with local topological changes, specifically with the merger of metallic lakes on the HB and semiconductor lakes on the CB. Near the major loop ends  $T_S$  and  $T_M$ , the global map consists of widely separated M- and S-lakes, respectively. In these regions, we expect to see nonhysteretic behavior, as was indeed observed in [8] and [9]. Consider now a small *backward* excursion from  $T_0$  on the HB. As the temperature decreases, some of the M-phase recedes and the S-phase grows, changing the geometry of the global two-phase map. However, topologically, the last formed M-link does not disappear immediately for the same kinetic reason. One has two S-regions that need to touch in order to wipe out the M-link. It takes a backward excursion of amplitude  $\Delta T^*$  to establish an S-link, and thus, disconnect the last M-link. So long as we are within  $\Delta T^*$ , i.e., stay on the same NHB, the area of S- and M-domains changes continuously, but the topology is stable and no new links are formed. Within the range of that stable or *frozen topology*  $\Delta T^* = \Delta T_{\text{NHB}}$ , the resistivity of NHB will be single-valued and its  $T$ -dependence will be controlled by the percolating semiconductor phase. This explains the appearance of NHB-s and why they have semiconducting slopes.

We can further attribute the observed TCR enhancement in some of the NHB-s, where TCR-s exceed the S-phase value [see Figs. 3 and 5], to a geometric area effect. We note that higher  $T$  implies increased area of the M-phase, even if no new links are formed. The smooth change in geometry discussed earlier produces an extra  $T$ -dependence, adding to the semiconductor slope within a NHB, so that the TCR is enhanced compared to its S-phase value. This effect will be observed in temperature

intervals, where this smooth change in geometry takes place (generally, within a major loop), being stronger when the rate of area redistribution  $dA_M/dT = -dA_S/dT$  is higher. As we can see from Figs. 3 and 5, peak values of TCR-s in NHB-s correspond to peak values of TCR-s on the major loop, and stronger (higher RR) overall transition produces correspondingly higher TCR-s in NHB-s. Both points are naturally explained within our qualitative picture. The aforementioned area redistribution rates are reflected in optical slopes, and correlation between these slopes and observed TCR peaks [8], [9] further supports this picture.

The percolation picture is also helpful in the qualitative understanding of why there must be a maximum in the area redistribution rate  $dA_M/dT$ . With the changing temperature, the boundary between S- and M-phases moves, each section of the boundary line advancing in the direction normal to this line at any given temperature. It is clear that the highest rate of change of the area of each phase will, therefore, occur when the boundary is the longest, i.e., near the percolation transition. If the picture is correct, then the observed peaks in TCR versus  $T$  in Figs. 3 and 5 occur right at the percolation transition, and is in fact a signature of this transition.

Finally, we see in Figs. 3 and 5 that at temperatures above the TCR peaks, i.e., above the percolation transition, TCR-s are quickly decreasing. Indeed, once the M-phase percolates, it is shorting out the S-phase, and such decrease is to be expected.

We recognize that some of the features of the qualitative picture presented earlier, such as the absence of intrinsic hysteresis in isolated microdomains, should be at this time treated as a hypothesis in need of additional experimental verification.

## VI. RESISTIVE MICROBOLOMETERS IN NHB REGIME

A detailed discussion of the NHB method in the context of IR visualization with resistive microbolometers (the UPPA technology) is given in [8]. Here, we only give a brief summary. Good quality, single-phase VO<sub>2</sub> films will replace mixed oxide VO<sub>x</sub> as sensor material in pixilated bolometric array. Despite using VO<sub>2</sub>, there is no hysteresis when the sensor array operates within a NHB. The NHB will be chosen on the basis of its desired resistance, which can be adjusted in a wide range in order to be matched to the readout circuit amplifier, and to be low enough to minimize both the noise and the Joule heating. The resistance will be 2–3 orders of magnitude smaller than the unacceptably high VO<sub>2</sub> resistance at 25 °C, while maintaining semiconducting TCR. The NHB will be also chosen so as to maximize TCR, which, as we have seen, varies between different NHB-s around the major loop, peaking at the percolation transition, with values up to 6% °C<sup>-1</sup> in samples with RR = 1400 and up to 21% °C<sup>-1</sup> in samples with RR = 8700. The operating temperature  $T_{OP}$  (i.e., the temperature at which the sensor array is stabilized awaiting the projected IR signal) will be chosen within a NHB, e.g., in the middle of the total NHB width  $\Delta T_{NHB}$ . Because of the hysteresis, the process of reaching  $T_{OP}$  starting from room temperature requires performing certain heating and cooling steps. Specifically, positioning an array at  $T_{OP}$  will require: on a HB, warming up to  $T_0$  and cooling down to  $T_{OP}$ ; on a

CB, warming up to above  $T_M$ , cooling down to  $T_0$ , and again warming up to  $T_{OP}$ .

The relatively narrow operating range ( $\approx 6$  °C in moderate, and  $\approx 2$  °C in strong transition samples), if it presents a problem, may be avoided altogether using an approach that requires no excursions from the operating temperature at all. Lerner [14] describes a heat balancing design in which an electrothermal feedback is used to maintain both the resistance and temperature at a constant value. Instead of directly detecting the temperature change by measuring changes in resistance, electric power is delivered to each detector pixel in such a way as to balance the heat absorbed from the target. As incoming radiation increases, the power needed to maintain a constant temperature decreases. The measure of said power difference provides information about heat input into the microbolometer from the scene. This approach was designed to avoid individual array calibration [14], but it also appears very well suited for our NHB regime.

## ACKNOWLEDGMENT

The authors would like to thank Dr. D. Westerfeld for developing LabVIEW-based automated resistivity measurement system and Dr. A. Subashiev for useful theoretical discussions.

## REFERENCES

- [1] R. Flannery and J. E. Miller, "Status of uncooled IR imagers," in *Proc. Infrared Imag. Syst.: Design, Anal., Model. Testing III, Proc. SPIE 1689*, 1992, pp. 379–395.
- [2] R. A. Wood and N. A. Foss, "Micromachined bolometer arrays achieve low-cost imaging," in *Proc. Laser Focus World*, Jun. 1993, pp. 101–106.
- [3] R. A. Wood, "Monolithic silicon microbolometer arrays," in *Semiconductors and Semimetals*, vol. 47. New York: Academic, 1997, pp. 43–121.
- [4] A. Rogalski, "Infrared detectors: Status and trends," *Progr. Quantum Electron.*, vol. 27, no. 2–3, pp. 59–210, Jan. 2003.
- [5] B. E. Cole, R. E. Higashi, and R. A. Wood, "Monolithic two-dimensional arrays of micromachined microstructures for infrared applications," *Proc. IEEE*, vol. 86, no. 8, p. 1679, Aug. 1998.
- [6] V. Yu. Zerov, Yu. V. Kulikov, V. N. Leonov, V. G. Malyarov, I. A. Khrebto, and I. I. Shaganov, "Features of the operation of a bolometer based on a vanadium dioxide film in a temperature interval that includes a phase transition," *J. Opt. Technol.*, vol. 66, no. 5, pp. 387–390, 1999.
- [7] M. Gurvitch, S. Luryi, A. Polyakov, and A. Shabalov. (2008, May). "Non-hysteretic branches inside the hysteresis loop in VO<sub>2</sub> films for focal plane array imaging bolometers," *Cond. Matt. ArXiv*. [Online]. Available: <http://arxiv.org/abs/0805.3566>
- [8] M. Gurvitch, S. Luryi, A. Polyakov, and A. Shabalov, "Non-hysteretic behavior inside the hysteresis loop of VO<sub>2</sub> and its possible application in infrared imaging," *J. Appl. Phys.*, vol. 106, pp. 104504-1–104504-15, 2009.
- [9] M. Gurvitch, S. Luryi, A. Polyakov, and A. Shabalov, "Treating the case of incurable hysteresis in VO<sub>2</sub>," in *Future Trends in Microelectronics: From Nanophotonics to Sensors and Energy*, S. Luryi, J. M. Xu, and A. Zaslavsky, Eds. Hoboken, NJ: Wiley Interscience, 2010.
- [10] F. J. Morin, "Oxides that show a metal-to-insulator transition at the Neel temperature," *Phys. Rev. Lett.*, vol. 3, pp. 34–36, 1959.
- [11] N. Mott, *Metal-Insulator Transitions*. London, U.K.: Taylor and Francis, 1997.
- [12] T. G. Lanskaya, I. A. Merkulov, and F. A. Chudnovskii, "Hysteresis effects at the semiconductor-metal phase transition in vanadium oxides," *Sov. Phys. Solid State*, vol. 20, no. 2, pp. 193–197, 1978.
- [13] C. N. Berglund and H. J. Guggenheim, "Electronic properties of VO<sub>2</sub> near the semiconductor-metal transition," *Phys. Rev.*, vol. 185, no. 3, pp. 1022–1033, 1969.
- [14] E. J. Lerner, "Uncooled IR detectors move into the mainstream," *Laser Focus World*, vol. 37, no. 5, pp. 201–204, 2001.



**Michael Gurvitch** received the Ph.D. degree in physics from the State University of New York (SUNY), Stony Brook, NY, in 1978.

In 1979, he joined Bell Laboratories, Murray Hill, NJ, and continued as a Member of the Technical Staff until 1989, where he was involved in research in superconductivity and physics of metals and, together with colleagues, developed a method for producing refractory Nb–Al–Nb Josephson junctions (the tri-layer method), which is still being used in all low-temperature superconducting circuits throughout the

World. In 1990, he joined as a Professor in the Department of Physics, Stony Brook University, Stony Brook. From 1990 to 1994, he was a Director of the Institute for Interface Phenomena, Stony Brook. He is also affiliated with New York State Center for Advanced Sensor Technology, SUNY. He has authored or coauthored more than 100 scientific papers. He holds five U.S. patents.



**Serge Luryi** (M'81–SM'85–F'90) received the Ph.D. degree in theoretical physics from the University of Toronto, ON, Canada, in 1978.

In 1980, he joined Bell Laboratories, Murray Hill, NJ, where he was involved in research in physics of semiconductor devices, until 1994, he was a Group Supervisor and a Distinguished Member of the Technical Staff. In 1994, he joined as a Chairperson in the Department of Electrical and Computer Engineering, Stony Brook University, Stony Brook. He is also the Founding Director of the New York State Center for

Advanced Sensor Technology, State University of New York (SUNY), Stony Brook, NY. He has authored or coauthored more than 230 scientific papers. He holds 47 U.S. patents.

Dr. Luryi was the Editor-in-Chief of IEEE TRANSACTIONS ON ELECTRON DEVICES during 1986–1990. In 1995, he organized the first international advanced research workshop on the “Future Trends in Microelectronics,” which has since grown into a celebrated series of conferences. The latest FTM meeting, “Future Trends in Microelectronics: Unmapped Roads,” was held in Sardinia, Italy, in June 2009. He was a Fellow of the American Physical Society in 1993 “for contributions to the theory of electron transport in low-dimensional systems and invention of novel electron devices,” and a Fellow of the Optical Society of America in 2007 “for outstanding and pioneering contributions to semiconductor optoelectronics, especially to the physics and photonic applications of low-dimensional semiconductor structures.” In 2003, he was appointed to the rank of Distinguished Professor by the Board of Trustees of SUNY. In 2006, he was recipient of the IEEE Papoulis Award for Excellence in Engineering and Technology Education with the citation: “For pioneering contributions to include entrepreneurial skills in engineering education on Long Island.”



**Aleksandr Polyakov** received the M.S. degree in physics from St. Petersburg State Technical University, St. Petersburg, Russia, in 1985, the B.S. degree in information systems (data communications), in 2004, and the M.S. degree in instruction technology from Touro College, Brooklyn, NY, in 2008.

In 1985, he had measured, analyzed, and computer-processed experimental results for semiconductor structures by Auger spectrometer, electron microscope, and mass spectrometer; installed, enhanced, operated, and maintained molecular beam epitaxy equipment at Scientific Research Company “Electron”, St. Petersburg.

In 1989, he joined North-West Polytechnic University, St. Petersburg, where he analyzed properties of diverse semiconductor structures and materials using laser optics, and as an Associate Professor in physics, where he taught mechanics, quantum mechanics, thermodynamics, optics, and electromagnetism. In 2003, he joined New York State Center for Advanced Technology, State University of New York (SUNY), Stony Brook, NY, where he is currently involved in applications of metal–semiconductor phase-transition in VO<sub>2</sub> films for microbolometer IR visualization technology. He is an Adjunct Professor at Touro College and SUNY, where he is teaching (regular and online) wide area networks, computer concepts and applications, calculus, and statistics courses. He has authored or coauthored 22 scientific papers. He holds 1 U.S. patent.



**Alexander Shabalov** received the M.S. degree in physics from the State University, Baku, Russia, in 1967, and the Ph.D. degree in physics and mathematics from the Institute of Physics, Baku, in 1972.

From 1968 to 1999, he was involved in the switching and memory effects in metal-oxide-metal and metal-oxide-semiconductor structures and multilayered optical coatings for Si and GaAs solar cells and IR detectors. He is currently a Senior Research Scientist with New York State Center for Advanced , State University of New York, Stony Brook, NY. His

research interests include the transition metal oxides, which exhibit electron correlation-driven metal–insulator transitions that in these materials should allow creating novel elementary electronic devices with advanced functionality.